

UWFormer: Underwater Image Enhancement via a Semi-Supervised Multi-Scale Transformer

Weiwen Chen^{1*}, Yingtie Lei^{1*}, Shenghong Luo¹, Ziyang Zhou², Mingxian Li², and Chi-Man Pun^{1†}

¹University of Macau, Macau, Macao

²Huizhou University, Huizhou, China

Abstract—Underwater images often exhibit poor quality, distorted color balance and low contrast due to the complex and intricate interplay of light, water, and objects. Despite the significant contributions of previous underwater enhancement techniques, there exist several problems that demand further improvement: (i) The current deep learning methods rely on Convolutional Neural Networks (CNNs) that lack the multi-scale enhancement, and global perception field is also limited. (ii) The scarcity of paired real-world underwater datasets poses a significant challenge, and the utilization of synthetic image pairs could lead to overfitting. To address the aforementioned problems, this paper introduces a Multi-scale Transformer-based Network called UWFormer for enhancing images at multiple frequencies via semi-supervised learning, in which we propose a Nonlinear Frequency-aware Attention mechanism and a Multi-Scale Fusion Feed-forward Network for low-frequency enhancement. Besides, we introduce a special underwater semi-supervised training strategy, where we propose a Subaqueous Perceptual Loss function to generate reliable pseudo labels. Experiments using full-reference and non-reference underwater benchmarks demonstrate that our method outperforms state-of-the-art methods in terms of both quantity and visual quality. The code is available at <https://github.com/leiyongtie/UWFormer>.

Index Terms—Underwater Image Enhancement, vision transformer, semi-supervised learning

I. INTRODUCTION

Underwater imaging is vital for the study of oceanic ecosystems, surveying marine resources and monitoring the environment. However, the quality of underwater images is often poor due to a combination of factors notably light scattering due to particle interactions, color cast caused by light wavelength absorption, turbidity from suspended particles, the influence of water depth and temperature, variations in light penetration, motion-induced blurring, and surface disturbances. As a result, underwater images often exhibit reduced clarity, distorted color balance and low contrast. To mitigate these challenges, various image enhancement techniques have been proposed. These techniques fall broadly into two categories: traditional methods and learning-based solutions [1]. Traditional underwater image enhancement methods often rely on mathematical models of the underwater environment and prior knowledge such as the medium transmission and the dark channel prior [2]–[6]. Additionally, they often require manual input of predefined parameters, which limits their adaptability

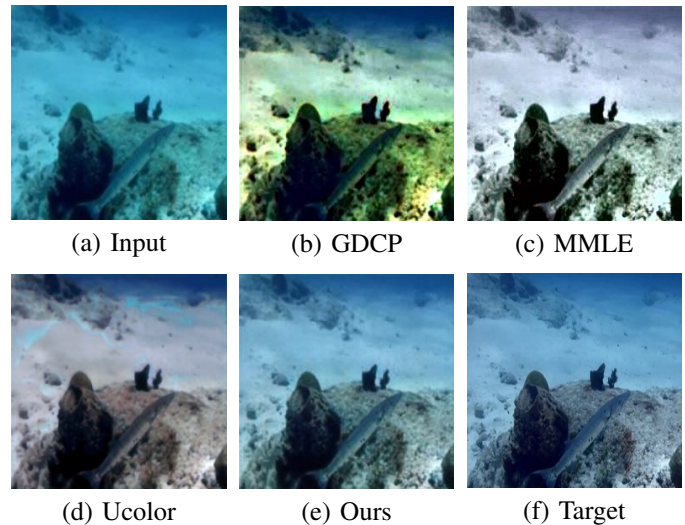


Fig. 1. The figure illustrates a comparison between (a) underwater image and (f) its enhanced version obtained from the EUVP dataset. Although (b),(c) traditional enhancement, and (d) deep learning models have been employed, they still manifest imperfections. By contrast, (e) our method effectively enhances the image.

to diverse and dynamic underwater environments, as depicted in Figure 1 (b).

Learning-based techniques and data-driven approaches seek to overcome these limitations by learning directly from data. Previous works [7]–[12] have demonstrated that improved performance can be achieved using deep learning and multi-frequency methods. However, most existing methods still rely on supervised learning, which requires large paired datasets for the model’s generalization. Although training on synthetically generated underwater images [13], [14] can be beneficial, it exhibits limitations in effectively capturing the intricate characteristics of real-world underwater scenes. Given the limited availability of large paired datasets for underwater image enhancement, it becomes imperative to harness the potential of features within unpaired datasets.

In addition, existing deep learning-based underwater enhancement techniques still rely on CNNs. Although CNNs excel at capturing local patterns and features within images through their convolutional and pooling layers, they might struggle with capturing long-range dependencies and global

* Equal contributions

† Corresponding author

context. The emergence of Vision Transformers [15] allows for the capture of both local and global information. This capacity for cross-positional interaction grants Vision Transformers an advantage in handling tasks requiring broader context and intricate relationships within images. Employing coarse-to-fine techniques constitutes a viable strategy for optimizing image processing efficiency and mitigating computational resource requirements. Another notable limitation of these prior works is the lack of multi-scale enhancement, which is particularly important as water interacts with light in a way that varies depending on the wavelengths of light. This causes different color spectra to undergo distinct attenuation rates during their passage through the water. Consequently, adopting a multi-scale methodology that optimizes for multiple wavelengths stands as a more precise strategy for encapsulating the intricate interplay of light, water, and objects. Such an approach has the potential to yield superior image enhancement. To address the aforementioned limitations, this paper introduces the following contributions:

- 1) We propose UWFormer, a novel semi-supervised Multi-scale Transformer for enhancing low-frequency features. UWFormer consists of two novel modules for underwater restoration: the Nonlinear Frequency-aware Attention module and the Multi-scale Fusion Feed-forward network. The incorporation of these two modules enables frequency-aware attention and varying receptive fields, which are shown to significantly improve the restoration performance.
- 2) We propose a unique semi-supervised framework for underwater settings. A Subaqueous Perceptual Loss function is used for generating positive pseudo labels. This approach allows the teacher’s output to provide reliable pseudo ground truth for the student model.
- 3) Extensive experiments on six benchmark datasets demonstrate that our UWFormer outperforms current state-of-the-art methods in terms of visual quality across various underwater scenarios.

II. RELATED WORK

A. Traditional Underwater Image Enhancement

Most of the traditional underwater image enhancement solutions are physics-based [16], such as Ancuti *et al.* [17] color correction and contrast enhancement method, rely on weight mapping and image combination techniques for the final output. Additionally, MMLE [18] utilizes locally adaptive contrast enhancement and color loss minimization to increase image clarity and enhance contrast. GDCP [19] proposed the generalized dark channel prior approach to restoring underwater images. Over the past few years, learning-based methods have emerged as powerful underwater image enhancement techniques.

B. Learning-based Underwater Image Enhancement

Recent years have seen rapid development of learning-based methods. Ucolor [20] uses a medium transmission-guided multicolor spatial embedding network to enhance vi-

sual quality effectively. Shallow-UWNet [21] is a lightweight neural network structure that enhances underwater images with fewer parameters. UWCNN [22] proposes an underwater image enhancement CNN model based on underwater scenes prior. PWRNet [23] utilizes a wavelet boost learning strategy to progressively enhance underwater images in both spatial and frequency domains. FuineGAN [10] enhances image brightness, contrast, and color balance in real-time, facilitating underwater target detection and identification. TOPAL [24] proposes a fusion network that adversarially and perceptually orients the target. UGAN [7] aims to enhance the performance of Autonomous Underwater Vehicles in vision-driven tasks.

III. METHODOLOGY

A. Overview

The overall architecture of the proposed UW-Former is illustrated in Figure 3. To enable multi-scale enhancement and save computational resources, we adopt lossless downsampling and reconstruction. We utilize the Discrete Wavelet Transform (DWT) and its inverse (IDWT) [25], [26] to enhance individual frequencies using distinct methods. Since high-frequency components, such as texture and edges, often undergo minor alteration [27], we use a simple residual network composed of Fast Fourier Convolutions to enhance these frequencies. Conversely, we introduce our proposed Transformer architecture to refine low-frequency components, which contain essential color information. This allows for fewer computing resources to be allocated to the high-frequency domain with lower variability, while dedicating more resources to the domain that requires more learning.

B. Transformer Architecture

The Vision Transformer model can effectively utilize self-attention to capture both global and local information concurrently, enabling the extraction of global features [28], [29]. This characteristic can be particularly advantageous for enhancing underwater images. Furthermore, coarse-to-fine strategies have been demonstrated to be effective for image enhancement [30]–[32] and other tasks [33]–[40]. Accordingly, we propose our Multi-scale Transformer, which stacks Transformers with multi-scale inputs and progressively refines image quality from bottom to top using the coarse-to-fine approach. This multi-scale architecture allows information in the image to flow through the network while tightly integrating low-level and high-level information into a UNet-like structure. The whole process is depicted in Figure 3.

More specifically, the UWFormer model contains four blocks for the feature extraction process at the start and four blocks for the feature reconstruction process at the end of the network. The model consists of a UNet architecture that has been optimized for multi-scale structures, with each block comprised of a Nonlinear Frequency-Aware Attention (NFA) layer and a Multi-Scale Fusion Feed-forward Network (MSFN). In the middle of the network are four encoders and three decoders, with a progressive increase in the number of blocks in each encoder and a progressive decrease

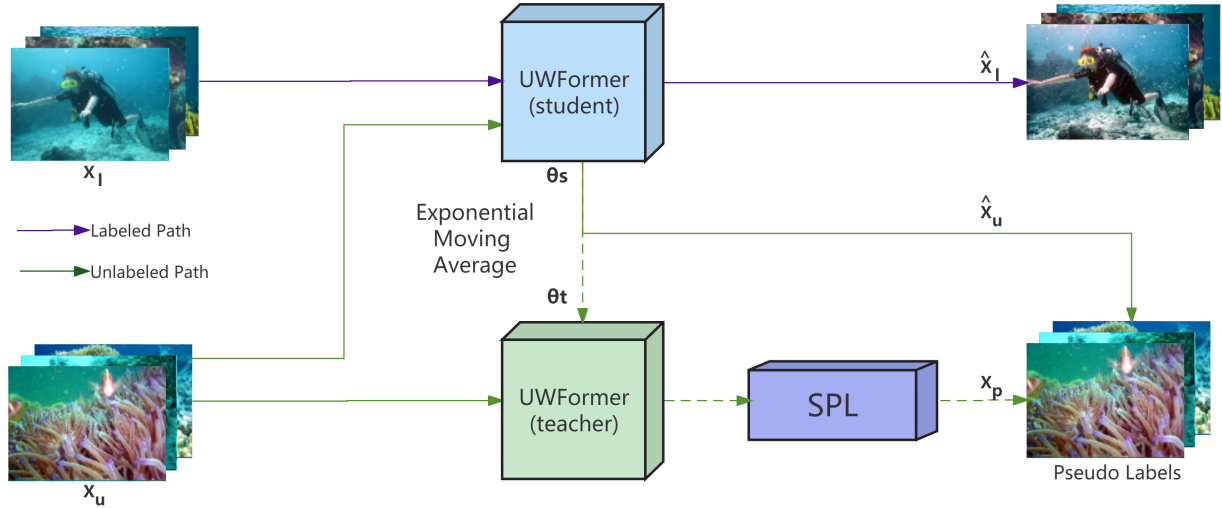


Fig. 2. Proposed underwater semi-supervised training strategy. Labeled images $X_l \in \mathbb{R}^{C \times H \times W}$ and unlabeled images $X_u \in \mathbb{R}^{C \times H \times W}$ are fed to: (i) the student model for training, and (ii) the teacher model for unlabeled prediction. The student model outputs labeled results \hat{X}_l and unlabeled results \hat{X}_u , with the \hat{X}_l converging using a supervised loss function. Note that the outputs of the teacher model are evaluated and updated in real-time using the proposed Subaqueous Perceptual Loss (SPL) to generate pseudo labels X_p . Finally, the unlabeled outputs of the student model \hat{X}_u are constrained by X_p using an unsupervised loss function. In this case, the weights of the student model are determined by both labeled data and unlabeled data.

in the number of blocks in each decoder. At each scale, we input $X_1 \in \mathbb{R}^{C \times H/2 \times W/2}$, $X_2 \in \mathbb{R}^{C \times H/4 \times W/4}$ and $X_3 \in \mathbb{R}^{C \times H/8 \times W/8}$ in addition to the original input image, $X \in \mathbb{R}^{C \times H \times W}$. Before being fed into each scale's encoder, the images undergo feature extraction using a convolution-based process and are then concatenated with the output of the previous encoder.

1) *Nonlinear Frequency-Aware Attention (NFA)*: Researchers like [41]–[44] have proposed to downsample and reconstruct feature maps in attention mechanism. However, relying on linear layers for learning image information may lead to the inability of the model to capture the non-linear patterns present in images, potentially leading to issues like overfitting and the presence of excessive parameters. To address this issue, we propose a new module called Nonlinear Frequency-aware Attention. In this module, we replace the conventional linear layers with simple convolutional layers and apply DWT and IDWT to enable lossless downsampling and reconstruction of the feature map. This results in a significant improvement of multi-scale enhancement for underwater scenarios and enhances the non-linear expressive power of the attention mechanism.

NFA processes the feature map $X \in \mathbb{R}^{C \times H \times W}$ through two pathways. The first pathway generates the Query $Q \in \mathbb{R}^{4C \times H \times W}$ by passing X through a 1×1 and 3×3 Depth-wise convolutional (DWConv) layer. In the second pathway, we concatenate the result of the DWT of X into four frequency domains and apply them to two sets of 1×1 and 3×3 convolutional layers to produce the Key $K \in \mathbb{R}^{16C \times H/2 \times W/2}$ and Value $V \in \mathbb{R}^{16C \times H/2 \times W/2}$. IDWT is also performed on the locally concatenated contextualized downsampled feature

X_c as a byproduct, which, according to wavelet theory, preserves every detail of the original input X . The Query, Key, and Value are subsequently reshaped into $\hat{Q} \in \mathbb{R}^{4C \times HW}$, $\hat{K} \in \mathbb{R}^{HW \times 4C}$, and $\hat{V} \in \mathbb{R}^{HW \times 4C}$, respectively, for the purpose of matrix multiplication. By implementing this process of DWT-Convolution-IDWT in the NFA, a more robust local contextualization with an enlarged receptive field is achieved.

Finally, we formulate the NFA as Eq. 1:

$$\begin{aligned} \text{NFA} &= \text{MultiHead}(Q, K, V, X^r), \\ \text{MultiHead}(Q, K, V, X^r) &= [\text{head}_0, \dots, \text{head}_j, X^r] W^O, \\ \text{head}_j &= \text{Attention}(Q_j, K_j, V_j) = \text{Softmax}\left(\frac{Q_j K_j^T}{\sqrt{D_h}}\right) V_j, \end{aligned} \quad (1)$$

where $[\cdot]$ stands for concatenation and W^O is the transformation matrix.

2) *Multi-Scale Fusion Feed-forward Network (MSFN)*: Inspired by FFC, which uses two channels for image processing, we propose the Multi-Scale Fusion Feed-forward Network. Similar to FFC, MSFN is a multi-scale structure comprising two connected pathways - a local pathway performing regular convolutions on specific input feature channels, and a global pathway, which operates larger convolutions in the global domain. Each path acquires diverse knowledge that is mutually complementary, allowing features to be improved at various scales across the network, facilitated by the exchange of information between them. Our design allows us to enhance features at multiple scales, a key benefit of MSFN over other architectures.

The MSFN model is designed to extract both detailed and global information from an underwater feature map $X \in$

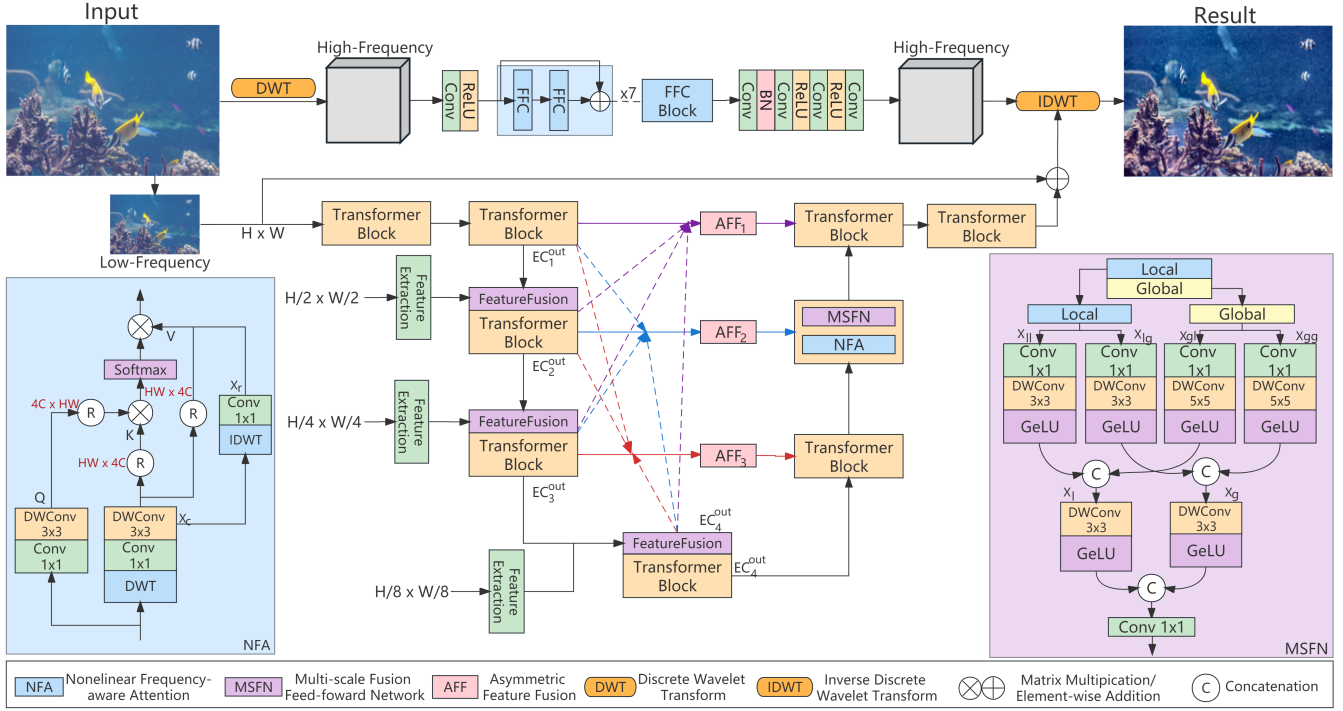


Fig. 3. Overall architecture of our proposed UWFormer. An input image $X \in \mathbb{R}^{C \times H \times W}$, it is first processed by DWT to produce three high-frequency images $\{X_{LH}, X_{HL}, X_{HH}\} \in \mathbb{R}^{C \times H \times W}$ and one low-frequency image $X_{LL} \in \mathbb{R}^{C \times H \times W}$. The three high-frequency images X_{LH}, X_{HL}, X_{HH} are then merged into a 9-channel image X_H and fed into a simple ResNet composed of FFC. The low-frequency part X_{LL} is fed into our MSFormer. Note that the X_{LL} at different scales are subjected to feature extraction and then fed into the MSFormer in a top-down way, where they are fused with the output of the previous encoder. Eventually, the output of the MSFormer $X_{LL}^{\hat{}}$ and the optimized image $X_H^{\hat{}}$ are subjected to IDWT to obtain the final result.

$\mathbb{R}^{C \times H \times W}$. Specifically, the local branch of MSFN employs regular 3×3 depth-wise convolution to extract detailed information, resulting in feature maps X_{l_l} and X_{l_g} with the same dimensions as X . On the other hand, the global branch of MSFN utilizes a larger 5×5 convolution kernel to capture more global information, resulting in feature maps X_g and X_{g_l} of the same size as X_l and X_{l_g} . To integrate the local and global information, the feature maps from both branches are combined in a cross-scale manner.

This process can be represented mathematically as shown in Equation 2, which yields a superior enhancement quality:

$$\begin{aligned}
 Y &= f_{1 \times 1} [\sigma(f_{3 \times 3}^{dwc}(X_l)), \sigma(f_{3 \times 3}^{dwc}(X_g))], \\
 X_l &= [\sigma(f_{3 \times 3}^{dwc}(X_{l_l})), \sigma(f_{5 \times 5}^{dwc}(X_{g_l}))], \\
 X_g &= [\sigma(f_{3 \times 3}^{dwc}(X_{l_g})), \sigma(f_{5 \times 5}^{dwc}(X_{g_g}))],
 \end{aligned} \quad (2)$$

where $\sigma(\cdot)$ indicates GeLU activation, $f_{1 \times 1}$ is 1×1 convolution, $f_{3 \times 3}^{dwc}$ and $f_{5 \times 5}^{dwc}$ denote 3×3 and 5×5 depth-wise convolution, $[\cdot]$ means concatenation.

C. Subaqueous Perceptual Loss

The limited availability of labeled underwater enhancement datasets necessitates the integration of unlabeled data to improve performance. Generally speaking, semi-supervised strategies are suitable for this scenario, but common semi-supervised strategies have not been optimized specifically

for underwater augmentation, which may result in ultimately unsatisfactory outcomes. To this end, we introduce a new Subaqueous Perceptual Loss in a special-designed semi-supervised training strategy to learn from both labeled and unlabeled data.

The Subaqueous Perceptual Loss is an underwater quality loss function defined in the CIELab [45], [46] color space that enables the teacher model to produce high-quality reliable pseudo labels, which can be written as Equation 3:

$$SPL = c_1 \times \sigma_c + c_2 \times c_l + c_3 \times \mu_s, \quad (3)$$

where c_1, c_2, c_3 are weighted coefficients, which are assigned the values 0.4680, 0.2745 and 0.2576 respectively; σ_c is the chroma standard deviation; c_l is the luminance contrast; μ_s is the average saturation.

The proposed UWFormer comprises two networks with matching structures, referred to as the teacher model and the student model [47]. The primary distinction between the two networks lies in how their weights are updated. More specifically, we utilize normal gradient descent to update the student's weights (θ_s), whereas the teacher's weights (θ_t) are updated based on the exponential moving average (EMA) of the student's weights. Through SPL, the outputs of the teacher model will significantly rectify the generation results of the student model and ultimately output desirable augmented underwater images.

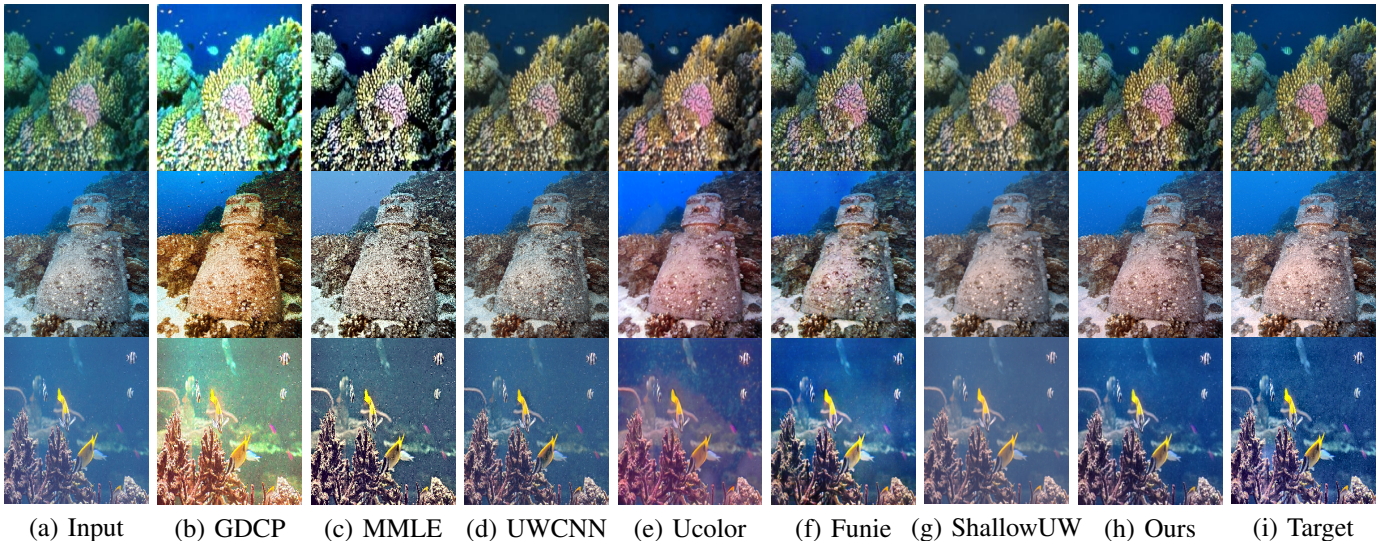


Fig. 4. A visual comparison of different image enhancement methods. Methods (b) and (c) show varying degrees of over-optimization, whereas methods (d) and (g) exhibit different degrees of under-optimization. Method (f) shows relatively satisfactory optimization results, yet some optimization defects can still be observed, such as the appearance of white blocks in the middle of the last row. However, our results (h) show superior visual results in terms of color tone and details, and are the closest to the target. The first two rows of images are sourced from EUVP, while the latter two rows are obtained from UIEB.

TABLE I
QUANTITATIVE RESULTS OF COMPARISONS WITH THE STATE-OF-THE-ART ON FULL-REFERENCE DATASETS. THE UPPER HALF OF THE TABLE IS THE COMPARISON EXPERIMENT, AND THE LOWER HALF SHOWS THE ABLATION EXPERIMENT. THE BEST PERFORMANCE IS MARKED IN BOLD.

Method	UIEB				EUVP			
	PSNR \uparrow	SSIM \uparrow	LPIPS \downarrow	UCIQE \uparrow	PSNR \uparrow	SSIM \uparrow	LPIPS \downarrow	UCIQE \uparrow
GDCP	14.72	0.745	0.213	0.443	13.10	0.638	0.329	0.427
MMLE	18.24	0.767	0.233	0.441	15.04	0.623	0.269	0.425
UWCNN	18.70	0.841	0.147	0.373	22.98	0.814	0.203	0.388
TOPAL	20.86	0.872	0.109	0.410	20.01	0.801	0.214	0.409
UGAN	21.16	0.787	0.149	0.438	21.58	0.787	0.201	0.424
FunieGAN	19.39	0.802	0.149	0.443	22.06	0.771	0.182	0.418
Ucolor	18.12	0.753	0.228	0.417	20.67	0.786	0.230	0.427
PWRNet	22.50	0.901	0.083	0.427	23.44	0.820	0.208	0.427
ShallowUW	17.66	0.660	0.390	0.354	22.55	0.802	0.205	0.379
UNet	17.93	0.792	0.200	0.389	22.19	0.802	0.212	0.384
W/O SPL	22.12	0.813	0.121	0.401	22.31	0.807	0.171	0.393
MDTA+MSFN	22.61	0.837	0.140	0.402	24.18	0.823	0.151	0.411
NFA+GDFN	22.32	0.831	0.144	0.439	22.56	0.740	0.191	0.425
Supervised	22.72	0.894	0.085	0.413	24.24	0.840	0.155	0.411
Ours	23.23	0.903	0.077	0.446	24.40	0.845	0.129	0.431

IV. EXPERIMENTS

A. Experiment Settings

In this section, we describe in detail the dataset, evaluation metrics and implementation details. It is worth noting that like previous works, we do not place emphasis on network speed since all the test data is 256×256 , so all the methods can generate results in a very short period of time.

1) *Dataset*: The training set for our experiment is made up of 2800 labeled image pairs and 2800 unlabeled images. The labeled dataset is randomly selected at a 5:2 ratio from EUVP [10] and UIEB [48]. The UIEB dataset consists of 890 real-world underwater images with accompanying ground truths. The unlabeled images are obtained in a ratio of 11:17 from the unpaired data in EUVPUN [10] and RUIE [49]. They represent a diverse range of underwater scenes, water types,

and lighting conditions, thus enhancing the generalization ability of our model.

For testing, we prepared two datasets: full-reference and no-reference. The full-reference dataset contains the remaining 90 paired images from UIEB and the remaining 200 paired images from EUVP. The no-reference dataset includes 1200 images from EUVPUN, full images from U45 [50], the remaining 1930 images from RUIE, and all images from UIEB-60 [48]. By incorporating different underwater scenarios, water types, and lighting conditions, these datasets can provide a comprehensive assessment of the model's performance.

2) *Evaluation Metrics*: Our study employs several full-reference evaluation metrics, including Peak Signal-to-Noise Ratio (PSNR), Structural Similarity Index (SSIM), and Learned Perceptual Image Patch Similarity (LPIPS) [51].

TABLE II

QUANTITATIVE RESULTS OF COMPARISONS WITH THE STATE-OF-THE-ART ON NO-REFERENCE DATASETS. THE UPPER HALF OF THE TABLE IS THE COMPARISON EXPERIMENT, AND THE LOWER HALF SHOWS THE ABLATION EXPERIMENT. THE BEST PERFORMANCE IS MARKED IN BOLD, WHILE THE SECOND-BEST PERFORMANCE IS UNDERLINED.

Method	EUVPUN		U45		RUIE		UIEB-60	
	UIQM \uparrow	UCIQE \uparrow						
GDCP	2.751	0.420	2.347	0.415	2.706	0.338	2.196	0.393
MMLE	2.737	0.419	2.599	0.423	2.805	0.345	2.197	0.395
UWCNN	2.812	0.374	3.151	0.380	2.580	0.245	2.427	0.338
TOPAL	2.812	0.414	3.165	0.392	2.871	0.287	2.728	0.373
UGAN	2.807	0.438	3.178	0.418	2.882	0.344	2.769	0.394
FunieGAN	2.804	0.440	3.202	0.417	2.802	0.361	2.879	0.401
Ucolor	2.824	0.430	3.042	0.421	2.607	0.275	2.424	0.395
PWRNet	2.806	0.418	3.222	0.423	2.822	0.338	2.700	0.388
ShallowUW	2.824	0.362	2.980	0.348	2.355	0.222	2.379	0.313
UNet	2.485	0.395	2.936	0.378	2.481	0.247	2.406	0.351
W/O SPL	2.718	0.417	3.074	0.403	2.757	0.329	2.726	0.367
MDTA+MSFN	2.723	0.408	3.101	0.401	2.686	0.315	2.711	0.361
NFA+GDFN	2.710	0.403	3.043	0.396	2.711	0.312	2.713	0.391
Supervised	2.658	0.419	3.136	0.403	2.781	0.314	2.718	0.377
Ours	2.831	0.442	3.227	0.440	2.891	<u>0.347</u>	<u>2.789</u>	0.416

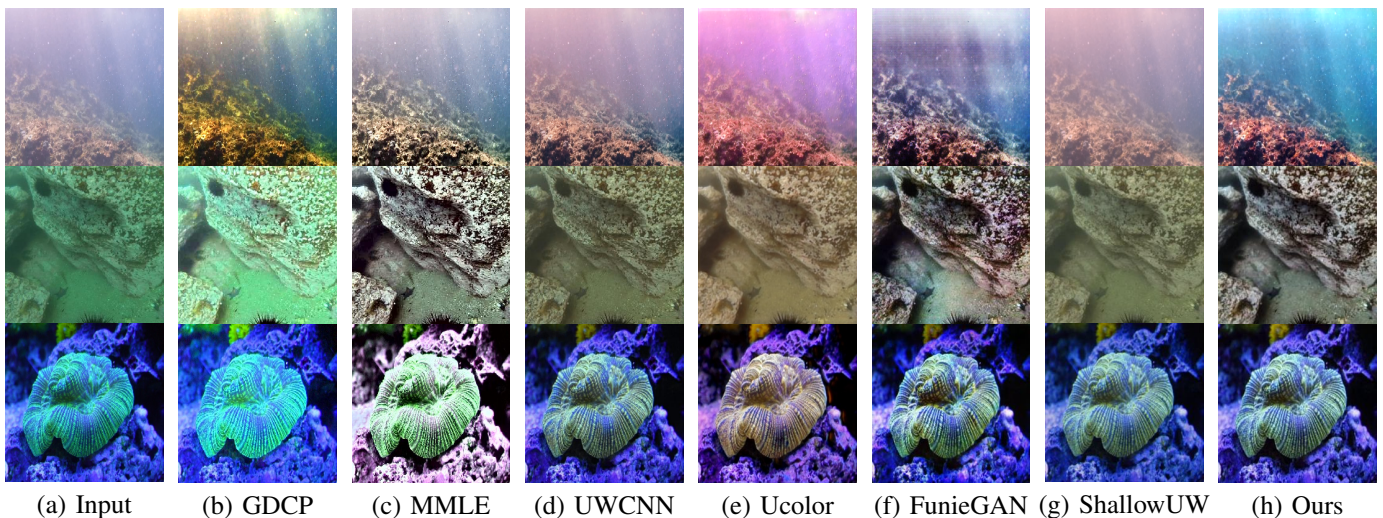


Fig. 5. Visual comparison of different image enhancement methods with no-reference datasets. It shows that methods (b), (c), and (e) exhibit considerable over-enhancement, while methods (d) and (g) do not fully enhance the images. Method (f) shows relatively satisfactory results albeit ambiguous optimization, such as ambiguous optimization in the first row and purple blotches in the third row. Our method (h) provides superior visual results in terms of color tone and details. The images in the rows from top to bottom, respectively originate from UIEB-60, U45, RUIE, and EUVPUN.

For no-reference evaluation metrics, we have selected two metrics. The first is the Underwater Image Quality Metric (UIQM) [52], which considers the unique degradation mechanisms and imaging characteristics of underwater images. The second metric is the Underwater Color Image Quality Evaluation (UCIQE) [45], which is a linear combination of colorfulness, saturation, and contrast. These metrics are chosen for their ability to accurately assess the quality of underwater images.

3) *Implementation Details*: Our model is implemented with PyTorch and trained using the Adam optimizer with default parameters on four NVIDIA RTX 8000. A batch size of 4 is used in training for 200 epochs, and the learning rate is reduced by a factor of 0.1 at epoch 100. The model is trained in a semi-supervised strategy for 200 epochs. Data augmentation

techniques included random flipping, rotation, cropping, and resizing.

B. Comparisons with State-of-the-Arts

We compared our UWFormer model with nine existing state-of-the-art methods, GDCP [19] and MMLE [18], UWCNN [22], TOPAL [24], UGAN [7], FunieGAN [10], Ucolor [20], PWRNet [23], and ShallowUW [21]. All methods have been retrained on our datasets with 200 epochs using their official implementations.

Table I presents the quantitative results of the full-reference datasets. It reveals that our UWFormer outperforms the existing methods in terms of both image similarity and visual quality in most metrics. Multi-scale Transformer architecture afforded a larger receptive field during supervised learning. This enabled superior performance over other methods in

color restoration and detail preservation. The superiority of our proposed method is also evident in Figure 4, where UWFormer achieves pleasing aesthetic outcomes, whereas the compared methods suffer from issues such as color cast and over-enhancement.

The quantitative results of the no-reference datasets are presented in Table II. Our UWFormer achieves the best performance for most metrics and ranks second in three metrics in the RUIE, and UIEB-60 datasets. Our proposed SPL function successfully achieved good performance in semi-supervised learning while maintaining supervised performance. Notably, generative models may hold an advantage for unsupervised tasks. We have provided visual comparisons in Figure 5, which demonstrate that our proposed method produces visually satisfying results, outperforming the existing methods.

C. Ablation Studies

We carry out ablation studies to assess the effectiveness of our proposed UWFormer approach by testing its individual components, and we replace NFA and MSFN with MDTA and GDFN since they are most commonly used mechanisms in Tranformer. These components are as follows:

- 1) **UNet**: A baseline;
- 2) **W/O SPL**: Let teacher model generate pseudo labels without SPL;
- 3) **MDTA+MSFN**: Replacing NFA with MDTA [53];
- 4) **NFA+GDFN**: Replacing MSFN with GDFN [53];
- 5) **Supervised**: The full-supervised training strategy without semi-supervision;
- 6) **Ours**: Our full UWFormer architecture with the semi-supervised training strategy.

The results of our ablation studies on full-reference and no-reference datasets are presented in Tables I and II, respectively. Our full version outperforms all other variants. We note that each module makes a significant contribution to the overall performance. Notably, each component proposed in this work contributed to improved performance.

The **baseline** experiments without our modules perform the worst. The **W/O SPL** represents the effectiveness of the proposed SPL loss function. Our **MDTA+MSFN** and **NFA+GDFN** experiments demonstrate the effectiveness of our NFA and MSFN, respectively. The **Supervised** experiment performs similarly to our full-version on the paired dataset but falls short on the no-reference metrics due to the absence of unlabeled data. In conclusion, our full-version model demonstrates excellent performance on both full-reference and no-reference datasets.

V. CONCLUSION

This paper presents UWFormer, a novel multi-scale Transformer-based network designed to enhance images across multiple frequencies using a semi-supervised learning approach. The proposed UWFormer architecture incorporates an underwater-specific design that enhances performance through the integration of a Nonlinear Frequency-aware Attention mechanism and a Multi-scale Fusion Feed-forward network.

Additionally, a new loss function Subaqueous Perceptual Loss is proposed to effectively guide the teacher model in generating pseudo labels. We conduct extensive experiments on full-reference and non-reference datasets to demonstrate that UWFormer outperforms existing methods both quantitatively and qualitatively.

ACKNOWLEDGMENT

This work was supported in part by the Huizhou Daya Bay Science and Technology Planning Project under Grant No.2020020003, in part by the Science and Technology Development Fund, Macau SAR, under Grant 0087/2020/A2 and Grant 0141/2023/RIA2.

REFERENCES

- [1] M. Yang, J. Hu, C. Li, G. Rohde, Y. Du, and K. Hu, "An in-depth survey of underwater image enhancement and restoration," *IEEE Access*, vol. 7, pp. 123 638–123 657, 2019. 1
- [2] P. L. Drews, E. R. Nascimento, S. S. Botelho, and M. F. M. Campos, "Underwater depth estimation and image restoration based on single images," *IEEE computer graphics and applications*, vol. 36, no. 2, pp. 24–35, 2016. 1
- [3] C.-Y. Li, J.-C. Guo, R.-M. Cong, Y.-W. Pang, and B. Wang, "Underwater image enhancement by dehazing with minimum information loss and histogram distribution prior," *IEEE Transactions on Image Processing*, vol. 25, no. 12, pp. 5664–5677, 2016. 1
- [4] X. Ding, Z. Liang, Y. Wang, and X. Fu, "Depth-aware total variation regularization for underwater image dehazing," *Signal Processing: Image Communication*, vol. 98, p. 116408, 2021. 1
- [5] G. Hou, J. Li, G. Wang, Z. Pan, and X. Zhao, "Underwater image dehazing and denoising via curvature variation regularization," *Multimedia Tools and Applications*, vol. 79, pp. 20 199–20 219, 2020. 1
- [6] D. Akkaynak and T. Treibitz, "Sea-thru: A method for removing water from underwater images," in *CVPR*. Computer Vision Foundation / IEEE, 2019, pp. 1682–1691. 1
- [7] C. Fabbri, M. J. Islam, and J. Sattar, "Enhancing underwater imagery using generative adversarial networks," in *2018 IEEE International Conference on Robotics and Automation (ICRA)*. IEEE, 2018, pp. 7159–7165. 1, 2, 6
- [8] X. Yu, Y. Qu, and M. Hong, "Underwater-gan: Underwater image restoration via conditional generative adversarial network," in *Pattern Recognition and Information Forensics: ICPR 2018 International Workshops, CVAUI, IWCF, and MIPPSNA, Beijing, China, August 20-24, 2018, Revised Selected Papers 24*. Springer, 2019, pp. 66–75. 1
- [9] P. Liu, G. Wang, H. Qi, C. Zhang, H. Zheng, and Z. Yu, "Underwater image enhancement with a deep residual framework," *IEEE Access*, vol. 7, pp. 94 614–94 629, 2019. 1
- [10] M. J. Islam, Y. Xia, and J. Sattar, "Fast underwater image enhancement for improved visual perception," *IEEE Robotics and Automation Letters*, vol. 5, no. 2, pp. 3227–3234, 2020. 1, 2, 5, 6
- [11] Z. Li, X. Chen, S. Wang, and C.-M. Pun, "A large-scale film style dataset for learning multi-frequency driven film enhancement," *arXiv e-prints*, pp. arXiv-2301, 2023. 1
- [12] Z. Li, X. Chen, C.-M. Pun, and X. Cun, "High-resolution document shadow removal via a large-scale real-world dataset and a frequency-aware shadow erasing net," *arXiv preprint arXiv:2308.14221*, 2023. 1
- [13] A. Shrivastava, T. Pfister, O. Tuzel, J. Susskind, W. Wang, and R. Webb, "Learning from simulated and unsupervised images through adversarial training," in *2017 IEEE Conference on Computer Vision and Pattern Recognition, CVPR 2017, Honolulu, HI, USA, July 21-26, 2017*. IEEE Computer Society, 2017, pp. 2242–2251. 1
- [14] S. E. Reed, Z. Akata, X. Yan, L. Logeswaran, B. Schiele, and H. Lee, "Generative adversarial text to image synthesis," in *Proceedings of the 33rd International Conference on Machine Learning, ICML 2016, New York City, NY, USA, June 19-24, 2016*, ser. JMLR Workshop and Conference Proceedings, M. Balcan and K. Q. Weinberger, Eds., vol. 48. JMLR.org, 2016, pp. 1060–1069. 1

- [15] A. Dosovitskiy, L. Beyer, A. Kolesnikov, D. Weissenborn, X. Zhai, T. Unterthiner, M. Dehghani, M. Minderer, G. Heigold, S. Gelly, J. Uszkoreit, and N. Houlsby, "An image is worth 16x16 words: Transformers for image recognition at scale," *ICLR*, 2021. 2
- [16] P. Sahu, N. Gupta, and N. Sharma, "A survey on underwater image enhancement techniques," *International Journal of Computer Applications*, vol. 87, no. 13, 2014. 2
- [17] C. Ancuti, C. O. Ancuti, T. Haber, and P. Bekaert, "Enhancing underwater images and videos by fusion," in *CVPR*. IEEE Computer Society, 2012, pp. 81–88. 2
- [18] W. Zhang, P. Zhuang, H.-H. Sun, G. Li, S. Kwong, and C. Li, "Underwater image enhancement via minimal color loss and locally adaptive contrast enhancement," *IEEE Transactions on Image Processing*, vol. 31, pp. 3997–4010, 2022. 2, 6
- [19] Yan-Tsung, Peng, Keming, Cao, Pamela, C., and Cosman, "Generalization of the dark channel prior for single image restoration," *IEEE Transactions on Image Processing*, vol. 27, no. 6, pp. 2856–2868, 2018. 2, 6
- [20] C. Li, S. Anwar, J. Hou, R. Cong, C. Guo, and W. Ren, "Underwater image enhancement via medium transmission-guided multi-color space embedding," *IEEE Transactions on Image Processing*, vol. 30, pp. 4985–5000, 2021. 2, 6
- [21] A. Naik, A. Swarnakar, and K. Mittal, "Shallow-uwnet: Compressed model for underwater image enhancement (student abstract)," in *AAAI*. AAAI Press, 2021, pp. 15 853–15 854. 2, 6
- [22] C. Li and S. Anwar, "Underwater scene prior inspired deep underwater image and video enhancement," *Pattern Recognition*, vol. 98, no. 1, p. 107038, 2019. 2, 6
- [23] F. Huo, B. Li, and X. Zhu, "Efficient wavelet boost learning-based multi-stage progressive refinement network for underwater image enhancement," in *Proceedings of the IEEE/CVF International Conference on Computer Vision*, 2021, pp. 1944–1952. 2, 6
- [24] Z. Jiang, Z. Li, S. Yang, X. Fan, and R. Liu, "Target oriented perceptual adversarial fusion network for underwater image enhancement," *IEEE Transactions on Circuits and Systems for Video Technology*, pp. 1–1, 2022. 2, 6
- [25] S. G. Mallat, "A theory for multiresolution signal decomposition: the wavelet representation," *IEEE transactions on pattern analysis and machine intelligence*, vol. 11, no. 7, pp. 674–693, 1989. 2
- [26] Z. Li, X. Chen, C.-M. Pun, and S. Wang, "Wavenhancer: Unifying wavelet and transformer for image enhancement," *arXiv preprint arXiv:2212.08327*, 2022. 2
- [27] J. Liang, H. Zeng, and L. Zhang, "High-resolution photorealistic image translation in real-time: A laplacian pyramid translation network," in *IEEE Conference on Computer Vision and Pattern Recognition, CVPR 2021, virtual, June 19–25, 2021*. Computer Vision Foundation / IEEE, 2021, pp. 9392–9400. 2
- [28] Z. Zhou, Y. Huo, G. Huang, A. Zeng, X. Chen, L. Huang, and Z. Li, "Qean: Quaternion-enhanced attention network for visual dance generation," *arXiv preprint arXiv:2403.11626*, 2024. 2
- [29] X. Chen, C.-M. Pun, and S. Wang, "Medprompt: Cross-modal prompting for multi-task medical image translation," *arXiv preprint arXiv:2310.02663*, 2023. 2
- [30] Z. Li, X. Chen, C.-M. Pun, and X. Cun, "High-resolution document shadow removal via a large-scale real-world dataset and a frequency-aware shadow erasing net," in *Proceedings of the IEEE/CVF International Conference on Computer Vision (ICCV)*, October 2023, pp. 12 449–12 458. 2
- [31] Z. Li, X. Chen, S. Wang, and C.-M. Pun, "A large-scale film style dataset for learning multi-frequency driven film enhancement," in *IJCAI*, E. Elkind, Ed. International Joint Conferences on Artificial Intelligence Organization, 8 2023, pp. 1160–1168. 2
- [32] S. Luo, X. Chen, W. Chen, Z. Li, S. Wang, and C.-M. Pun, "De-vignet: High-resolution vignetting removal via a dual aggregated fusion transformer with adaptive channel expansion," *arXiv preprint arXiv:2308.13739*, 2023. 2
- [33] W. Liu, X. Shen, C.-M. Pun, and X. Cun, "Explicit visual prompting for low-level structure segmentations," in *Proceedings of the IEEE/CVF Conference on Computer Vision and Pattern Recognition*, 2023, pp. 19 434–19 445. 2
- [34] Q. Zuo, J. Hu, Y. Zhang, J. dong Pan, C. Jing, X. Chen, X. Meng, and J. Hong, "Brain functional network generation using distribution-regularized adversarial graph autoencoder with transformer for dementia diagnosis," *Computer Modeling in Engineering & Sciences*, vol. 137, pp. 2129–2147, 2023. 2
- [35] W. Liu, X. Cun, C.-M. Pun, M. Xia, Y. Zhang, and J. Wang, "Coordfill: Efficient high-resolution image inpainting via parameterized coordinate querying," in *Proceedings of the AAAI Conference on Artificial Intelligence*, vol. 37, no. 2, 2023, pp. 1746–1754. 2
- [36] W. Liu, X. Shen, H. Li, X. Bi, B. Liu, C.-M. Pun, and X. Cun, "Depth-aware test-time training for zero-shot video object segmentation," *arXiv preprint arXiv:2403.04258*, 2024. 2
- [37] H. Li and C.-M. Pun, "Cee-net: complementary end-to-end network for 3d human pose generation and estimation," in *Proceedings of the AAAI Conference on Artificial Intelligence*, vol. 37, no. 1, 2023, pp. 1305–1313. 2
- [38] —, "Monocular robust 3d human localization by global and body-parts depth awareness," *IEEE Transactions on Circuits and Systems for Video Technology*, vol. 32, no. 11, pp. 7692–7705, 2022. 2
- [39] C. Jing, Y. Shen, S. Zhao, Y. Pan, C. P. Chen, B. Lei, and S. Wang, "Estimating addiction-related brain connectivity by prior-embedding graph generative adversarial networks," *IEEE Transactions on Cybernetics*, 2024. 2
- [40] C. Jing, C. Gong, Z. Chen, B. Lei, and S. Wang, "Ta-gan: transformer-driven addiction-perception generative adversarial network," *Neural Computing and Applications*, vol. 35, no. 13, pp. 9579–9591, 2023. 2
- [41] T. Yao, Y. Pan, Y. Li, C.-W. Ngo, and T. Mei, "Wave-vit: Unifying wavelet and transformers for visual representation learning," in *Computer Vision—ECCV 2022: 17th European Conference, Tel Aviv, Israel, October 23–27, 2022, Proceedings, Part XXV*. Springer, 2022, pp. 328–345. 3
- [42] X. Chen, B. Lei, C.-M. Pun, and S. Wang, "Brain diffuser: An end-to-end brain image to brain network pipeline," in *Pattern Recognition and Computer Vision (PRCV)*, 2023, pp. 16–26. 3
- [43] G. Huang, X. Chen, Y. Shen, and S. Wang, "Mr image super-resolution using wavelet diffusion for predicting alzheimer's disease," in *International Conference on Brain Informatics (BI)*, 2023, pp. 146–157. 3
- [44] T. Zhou, X. Chen, Y. Shen, M. Nieuwoudt, C.-M. Pun, and S. Wang, "Generative ai enables eeg data augmentation for alzheimer's disease detection via diffusion model," in *2023 IEEE ISPCE-ASIA*, 2023, pp. 1–6. 3
- [45] M. Yang and A. Sowmya, "An underwater color image quality evaluation metric," *IEEE Transactions on Image Processing*, vol. 24, no. 12, pp. 6062–6071, 2015. 4, 6
- [46] W. G. Backhaus, R. Kliegl, and J. S. Werner, *Color vision: Perspectives from different disciplines*. Walter de Gruyter, 2011. 4
- [47] A. Tarvainen and H. Valpola, "Mean teachers are better role models: Weight-averaged consistency targets improve semi-supervised deep learning results," in *Advances in Neural Information Processing Systems 30: Annual Conference on Neural Information Processing Systems 2017, December 4–9, 2017, Long Beach, CA, USA*, I. Guyon, U. von Luxburg, S. Bengio, H. M. Wallach, R. Fergus, S. V. N. Vishwanathan, and R. Garnett, Eds., 2017, pp. 1195–1204. 4
- [48] C. Li, C. Guo, W. Ren, R. Cong, J. Hou, S. Kwong, and D. Tao, "An underwater image enhancement benchmark dataset and beyond," *IEEE Transactions on Image Processing*, vol. 29, pp. 4376–4389, 2019. 5
- [49] R. Liu, X. Fan, M. Zhu, M. Hou, and Z. Luo, "Real-world underwater enhancement: Challenges, benchmarks, and solutions under natural light," *IEEE Transactions on Circuits and Systems for Video Technology*, vol. 30, no. 12, pp. 4861–4875, 2020. 5
- [50] H. Li, J. Li, and W. Wang, "A fusion adversarial underwater image enhancement network with a public test dataset," *ArXiv preprint*, vol. abs/1906.06819, 2019. 5
- [51] R. Zhang, P. Isola, A. A. Efros, E. Shechtman, and O. Wang, "The unreasonable effectiveness of deep features as a perceptual metric," in *2018 IEEE Conference on Computer Vision and Pattern Recognition, CVPR 2018, Salt Lake City, UT, USA, June 18–22, 2018*. IEEE Computer Society, 2018, pp. 586–595. 5
- [52] K. Panetta, C. Gao, and S. Agaian, "Human-visual-system-inspired underwater image quality measures," *IEEE Journal of Oceanic Engineering*, vol. 41, no. 3, pp. 541–551, 2015. 6
- [53] S. W. Zamir, A. Arora, S. Khan, M. Hayat, F. S. Khan, and M.-H. Yang, "Restormer: Efficient transformer for high-resolution image restoration," in *Proceedings of the IEEE/CVF conference on computer vision and pattern recognition*, 2022, pp. 5728–5739. 7